A Theoretical Study of the Epoxidation of Olefins by Peracids

Shinichi Yamabe,*,† Chisako Kondou,† and Tsutomu Minato‡

Department of Chemistry, Nara University of Education, Takabatake-cho, Nara 630, Japan, and Institute for Natural Science, Nara University, 1500 Misasagi-cho, Nara 631, Japan

Received September 7, 1995 (Revised Manuscript Received October 31, 1995⊗*)*

For the parent reacting system, HCOOOH + CH_2=CH_2 → HCOOH + ethylene oxide, the overall potential energy surface has been determined using *ab initio* methods. The oxygen-addition transition state is found to be remarkably similar to that deduced experimentally. The O−H bond is retained in the transition state. Reasonable kinetic isotopic effects are obtained theoretically. The transition state leads to an unprecedented transient intermediate. That intermediate is converted to a hydrogen-bonded system between ethylene oxide and formic acid. Substituent effects on transition-state geometries are small, but the effects on activation energies are large.

I. Introduction

The epoxidation of olefins by peracids (Prilaschajew reaction) is a familiar and synthetically useful reaction.[1] In spite of extensive studies, its reaction mechanism is not yet settled. Classically, Bartlett's mechanism suggested the symmetrical transfer of an oxygen atom to the olefin from the internally hydrogen bonded peracid monomer (Scheme 1).[2] Bartlett's cyclic planar concerted mechanism is reasonable in view of experimental observations.[3,4]

(1) The reaction is second order.

(2) The reaction occurs readily even in nonpolar solvents.

(3) The oxygen addition is stereospecific.

(4) The reaction is insensitive to steric effects.

Hammett $\sigma-\rho$ studies[5] and kinetic isotope effects led to a plausible transition-state (TS) structure of peracid epoxidation. Chart 1 shows a proposed transition-state structure for epoxidation of arylethenes with substituted perbenzoic acids. Important findings related to the transition-state structure in Chart 1[6] are as follows.

(1) Hammett ρ values indicate that peracids are electron acceptors and olefins are donors.

(2) Isotopic effects (in square brackets) show that the O−H bond is not weakened significantly in the transition state.

(3) C_6 is an sp^3 carbon due to the predominant C_6-O_4 bond formation in the transition state.

(4) *The $O_4\cdots C_7$ bond is not yet formed in the transition state, and C_7 has an sp^2 nature.*

(5) *The transition state should have an unsymmetrical, open-chain structure.*

The transition-state structure has been proposed as a summary of isotope effects, stereospecificity, Hammett correlation and solvent effects in Chart 1.[6] The peracid

Scheme 1

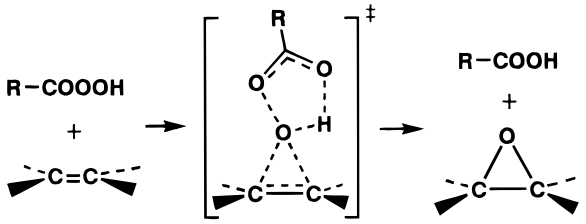

Chart 1

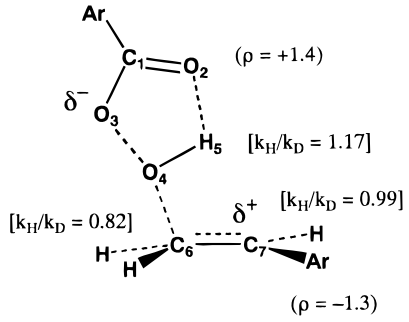

epoxidation is rather insensitive to solvent effects, and its reactivity should correlate closely with the electronic structure of the transition state. It is of mechanistic interest to examine whether theoretical studies agree with Bartlett's mechanism in Scheme 1 or the deduced transition-state structure in Chart 1.

There are only two studies which have used *ab initio* calculations to study the present reaction.[7,8] The first theoretical work reported and compared five approximate transition-state models using minimal basis sets (STO-2G and STO-4G).[7] In the second work, the transition-state structure was determined with more reliable computational methods (e.g., MP2/6-31G*).[8] Unfortunately, this transition-state structure is a symmetric-bridged type and is incompatible with the experimentally deduced structure in Chart 1. Thus, it is still uncertain whether the reaction is really concerted and the transition-state structure in Chart 1 is correct.

In order to shed light on the reaction mechanism, we have carried out *ab initio* calculations. First, the overall potential energy surface of the parent reaction, HCOOOH

† Nara University of Education.

‡ Nara University.

⊗ Abstract published in *Advance ACS Abstracts,* January 1, 1996.

(1) For reviews of key references, see: (a) Rebek, J., Jr. *Heterocycles* **1981**, *15*, 517. (b) Mimoun, H. *Angew. Chem., Int. Ed. Engl.* **1982**, *21*, 734.

(2) Bartlett, P. D. *Rec. Chem. Prog.* **1957**, *18*, 111.

(3) March, J. *Advanced Organic Chemistry, 3rd ed.*; John Wiley & Sons: New York, 1985.

(4) Sea, K. J.; Kim, J.-S. *J. Am. Chem. Soc.* **1992**, *114*, 3044.

(5) (a) Lynch, B. M.; Pausacker, H. *J. Chem. Soc.* **1955**, 1525. (b) Ogata, Y.; Sawaki, Y.; Inoue, H. *J. Org. Chem.* **1973**, *38*, 1044. (c) Ishii, Y.; Inamoto, Y. *Kogyo Kagaku Zasshi* **1960**, *63*, 765.

(6) Hanzlik, R. P.; Shearer G. O. *J. Am. Chem. Soc.* **1975**, *97*, 5231.

(7) Plesnicar, B.; Tasevski, M.; Azman, A. *J. Am. Chem. Soc.* **1978**, *100*, 743.

(8) Bach, R. D.; Owensby, A. L.; Gonzalez, C.; Schlegel, H. B.; McDouall, J. J. W. *J. Am. Chem. Soc.* **1991**, *113*, 2338.

0022-3263/96/1961-0616$12.00/0

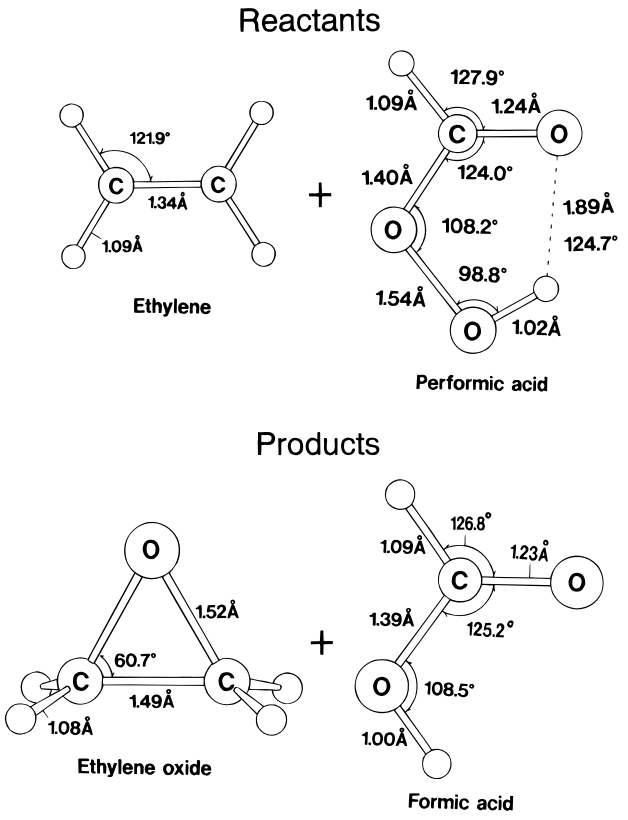

Figure 1. Geometries of reactants and products optimized with MP2/3-21G. Empty circles represent hydrogen atoms.

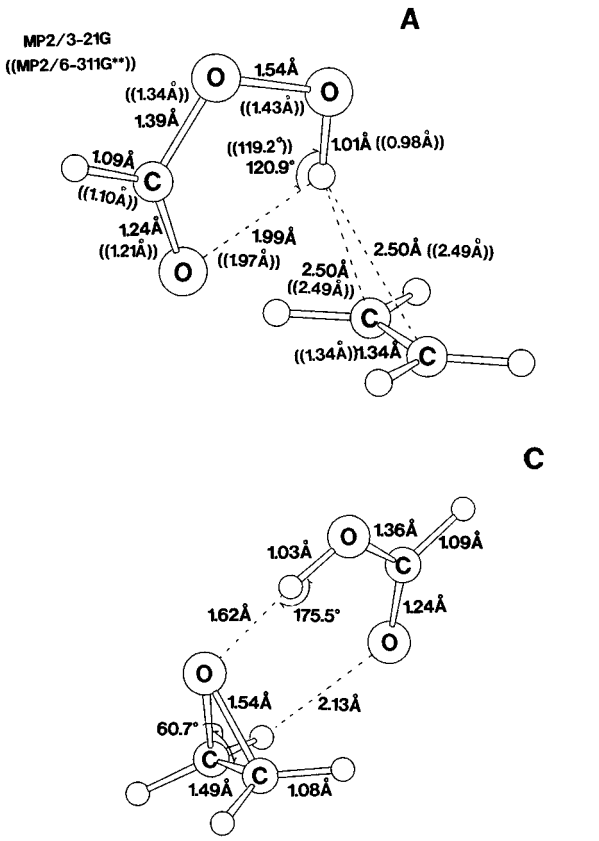

Figure 2. Intermediates A (prior to TS1) and C (after TS2) formed by association of reactants and products, respectively. MP2/3-21G and MP2/6-311G** geometric data ((in double parentheses)) are shown.

+ $CH_2{=}CH_2$, was investigated. Second, substitution effects on both the peracid and olefin were examined. Particular interest was paid to the concertedness of the reaction where O−O and O−H bonds are cleaved in the transition state.

II. Method of Calculations

Ab initio calculations were performed with GAUSSIAN 92.[9] Second-order Møller−Plesset perturbation methods using 3-21G, 6-31G*, and 6-311G** basis sets (MP2/3-21G, MP2/6-31G*, and MP2/6-311G**) were used in geometry optimizations. The validity of the MP2 methods was also checked for the transition state of the rate-determining step by the four-electron and four-orbital active space SCF wavefunction with the 3-21G basis set, CASSCF(4,4)/3-21G.

All the stationary points were examined with vibrational analyses to judge whether they were stable species or transition states.[10] The transition state was characterized by a single imaginary frequency.

Single-point energy calculations were carried out with the full fourth-order Møller−Plesset perturbation using the 6-31G* and 6-311G** basis sets on the geometries optimized by the MP2/3-21G method (MP4(SDTQ)/6-31G*//MP2/3-21G and MP4(SDTQ)/6-311G**//MP2/3-21G). The frozen core option was applied to all MP2 and MP4 calculations. Full computational data are shown in the Supporting Information.

III. Results of Calculations

Figure 1 shows the geometries of the reactants and products. In performic acid, the angle of the internal hydrogen bond is 124.7°. As the reaction occurs, the proton should migrate. Since ideal hydrogen bonds are linear, the 124.7° angle is unfavorable for intramolecular proton transfer.

Figure 2 shows bound species of reactants and products obtained here. The association intermediate A is a long-range complex and is of intermolecular interaction. On the other hand, the hydrogen-bonded intermediate C is strongly bound owing to the short O···H (=1.62 Å) distance.

(9) Frisch, M. J.; Trucks, G. W.; Head-Gordon, M.; Gill, P. M. W.; Wong, M. W.; Foresman, J. B.; Johnson, B. G.; Schlegel, H. B.; Robb, M. A.; Replogle, E. S.; Gomperts, R.; Andres, J. L.; Raghavachari, K.; Binkley, J. S.; Gonzalez, C.; Martin, R. L.; Fox, D. J.; DeFrees, D. J.; Baker, J.; Stewart, J. J. P.; Pople, J. A. *Gaussian 92, Revision C*; Gaussian Inc.: Pittsburgh, PA, 1992.

(10) In view of the experimantally deduced asymmetric structure in Chart 1, TS1 was searched for in the following way. First, fixing the distance between the hydroxyl oxygen atom (O_4 in Figure 3) in HCOOOH and the methylene carbon (C_6 in Figure 3) in ethylene, we optimized partially all other geometric parameters. This partial optimization was repeated with respect to various fixed $O_4\cdots C_6$ distances. An energy maximum was found along the $O_4\cdots C_6$ distance abscissa. This maximum point is an approximate transition state, and the optimization job is initiated by the use of this geometry with the keyword option, opt = (ts, noeig, calcfc). If the partial optimization is rough in locating the saddle point, TS1, the transition-state search will be unsuccessful. The precise partial optimization is required with IOP (1/8 = 1). It was very difficult to determine the second transition state (TS2 in Figure 5), because the reaction B → C (see Figure 6) is significantly exothermic and any transition-state search tends to lead to the stable intermediate C. This "early" transition state has a geometry close to that of the intermediate B. The geometry of B was distorted carefully with the increment of the $O_4\cdots C_6$ distance (see Figure 4), 0.001 Å. By this 0.001 Å increment partial optimization and subsequent transition-state search, we succeeded in determining the geometry of TS2. In general, when a reaction is heavily exothermic, its saddle point should be searched for by quite a small displacement of the reactant geometry.

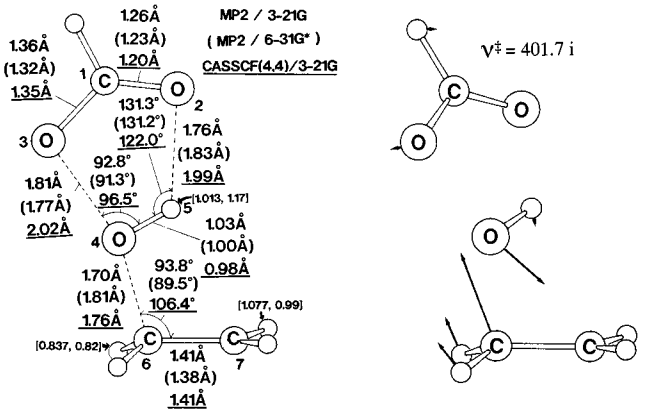

Figure 3. First transition-state (TS1) geometry optimized with three methods, MP2/3-21G, MP2/6-31G* (in parentheses), and CASSCF(4,4)/3-21G (underlined). For three hydrogen atoms, theoretical and experimental kinetic isotope effect values are shown on the left and right sides of the brackets, respectively. The experimental values are taken from ref 6. The reaction-coordinate vector corresponding to the sole imaginary frequency (MP2/3-21G, numerical calculations of the second derivatives) is also sketched.

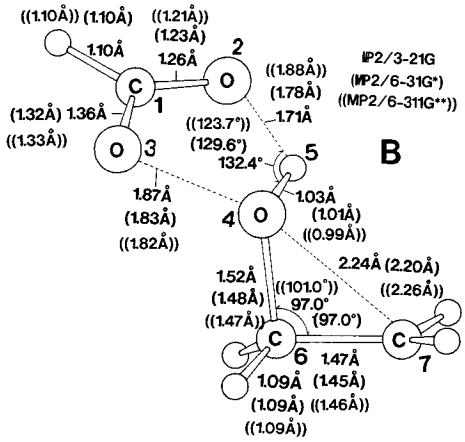

Figure 4. The geometry of the intermediate B (after TS1) optimized with MP2/3-21G, MP2/6-31G* (in parentheses), and MP2/6-311G** ((in double parentheses)) methods.

As the reaction proceeds from intermediate A, it arrives at the transition state, TS1, shown in Figure 3. The structure of TS1 is fully consistent with the experimental predictions of the asymmetry of the oxygen transfer TS. That is, the transition state has an unsymmetrical structure, and the O−H bond is not weakened in the transition state.

Since this is the transition state of the rate-determining step, three computational methods were used to check it. First, the basis set (3-21G and 6-31G*) dependence for the second-order Møller−Plesset (MP2) wave function was examined. Almost the same transition-state geometries were obtained by the two methods. The energy difference between MP2/6-31G*//MP2/3-21G and MP2/6-31G*//MP2/6-31G* is within 1 kcal/mol, and so the MP2/3-31G geometry optimization is acceptable also energetically. The CASSCF(4,4)/3-21G TS1 geometry was found to be similar to those of MP2/3-21G and MP2/6-31G* (Figure 3). The energy difference between MP2/6-31G*//CASSCF(4,4)/3-21G and MP2/6-31G*//MP2/6-31G* is somewhat large (10 kcal/mol). Although CASSCF geometry optimizations are more desirable, the substituted systems (in Figures 7 and 8) are too large to calculate under the present computational capability. In view of the qualitative similarity of three geometries, the potential energy surface of the parent reaction, HCOOOH + CH_2=CH_2, and substituent effects on the rate-determining step were investigated using the MP2/3-21G method.

The computed kinetic isotopic effect k_H/k_D was evaluated using Eyring's transition-state theory.[11] The values on the left side in square brackets are found to agree fairly well with observed ones on the respective right sides (see also Chart 1). The reaction-coordinate vector indicates C_6−O_4 bond completion. Little O−H bond scission is indicated in the vector.

From TS1, the intrinsic reaction coordinate[12] was traced. The reverse path is directed to the intermediate A. The forward path leads to an unprecedented intermediate B (shown in Figure 4). In B, a HCOO···H_2C-(OH)−CH_2 interacting system, one C−O bond is almost formed. The HCOO moiety is anionic (−0.27 in TS1 and −0.35 in B by RHF/3-21G density) relative to that of A.

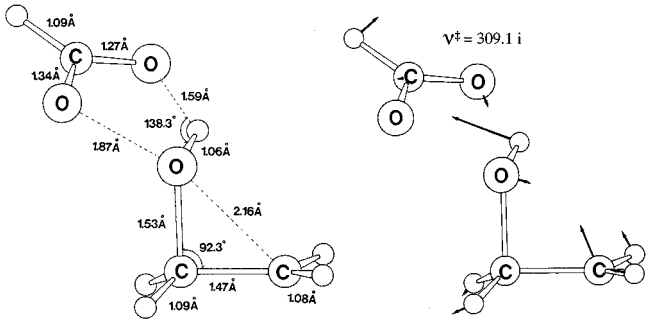

Figure 5. Geometry of the second transition state (TS2, after the intermediate B). The reaction-coordinate vector corresponding to the sole imaginary frequency is also sketched.

In B, the O−H bond is still short (1.03 Å or 1.01 Å). Here, the concertedness is violated by this retention of the O−H bond after TS1. B is thought to be unstable and transient, because O_4−C_7 and O_2−H_5 bonds are not yet completed. In Figure 4, as was made in Figure 3, the MP2/3-21G geometry of B was compared with the MP2/6-31G* one. The similarity of the geometries demonstrates that MP2/3-21G is acceptable in describing the transient species. The intermediate B is followed by the second transition state, TS2, shown in Figure 5. The geometry of TS2 is found to be almost the same as that of B except that the O···H distance is shorter in the former. The reaction-coordinate vector indicates both the closure of the epoxide ring and proton transfer. The vector leads to the hydrogen-bonded intermediate C shown in Figure 2.

(11) The second-order rate constant k_2 is given below according to the transition state theory

$$k_2 = (kT/h)(RT/p)\exp(-\Delta G^{\ddagger}/RT)$$

where k is the Bolzmann constant, T is the temperature (K), h is the Planck constant, R is the gas-phase constant, p is the pressure, and $-\Delta G^{\ddagger}$ is the activation free energy. Gibbs free energies can be obtained as the sum of the internal energy U (i.e., "SUM of HARTREE-FOCK AND THERMAL ENERGY" in the thermochemistry output of GAUSSIAN 92) and the entropy S, $G = U - TS + RT$. Here, the term RT is needed to convert the internal energy U to the enthalpy, $H = U + pv$ (1 mol). In the frequency job, any hydrogen atoms can be replaced by deuterium atoms, by specifying freq = (readfc, readiso). Thus, k_2(H) and k_2(D) can be calculated separately by obtaining respective free-energy changes (TS1−reactants), $\Delta G^{\ddagger}$(H) and $\Delta G^{\ddagger}$(D). The ratio k_2(H)/k_2(D) is shown in Figure 3.

(12) (a) Fukui, K. *J. Phys. Chem.* **1970**, *74*, 4161. (b) Gonzalez. C.; Schlegel, H. B. *J. Phys. Chem.* **1989**, *90*, 2154.

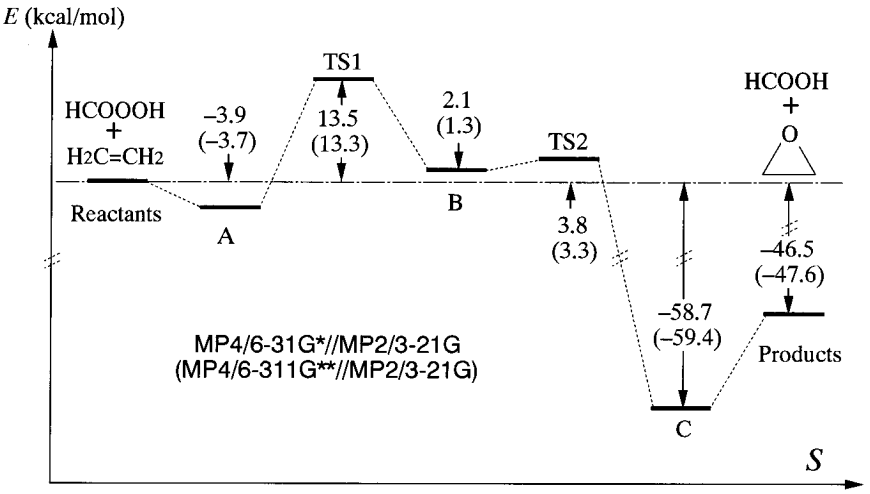

Figure 6. Potential-energy diagram of the parent olefin epoxidation calculated with MP4(SDTQ)/6-31G*//MP2/3-21G and (MP4-(SDTQ)/6-311G**//MP2/3-21G). When the MP2/3-21G thermal energy is taken into account, the activation energy (reactants−TS1) is +1.02 kcal/mol larger than those shown in this figure.

Figure 6 shows the potential-energy profile.[13] When performic acid encounters ethylene, a weakly-bound intermediate A (Figure 2) is generated. Due to the shallow energy minimum, A is undetectable under normal conditions. Next, TS1 (Figure 3) is in the rate-determining step with an activation energy of 13.5 (13.3) kcal/mol. This energy is somewhat smaller than the reported theoretical ones, 15.8,[7] 15.7, and 16.5[8] kcal/mol. The energy of intermediate B (Figure 4) is calculated to be 2.1 (1.3) kcal/mol less than that of the reactants. B is followed by TS2 (Figure 5) with a 1.7 kcal/mol (=3.8−2.1 shown in Figure 6) activation energy. After TS2, C (Figure 2) is generated with a large negative energy relative to the reactants, −58.7 (−59.4) kcal/mol. Since the step B → C is quite exothermic, the excess energy will be used to decompose C into products.[14] The reaction energy, i.e., the difference of energies between the reactants and the products, is −46.5 (−47.6) kcal/mol. This is in excellent agreement with the experimental one, −46.2 kcal/mol.[7] Figure 6 demonstrates that the peracid epoxidation of olefins is *not* concerted.

Figure 7 shows substituent effects of the peracid on TS1. As the substituent changes, X = NH2 → Me → H → CN, activation energies decrease considerably. The change, of course, reflects the electrophilic character of peracids, i.e., the Hammett $\rho = +1.4$ in Chart 1. In spite of the large energy change, surprisingly, the TS1 geometries are nearly the same.

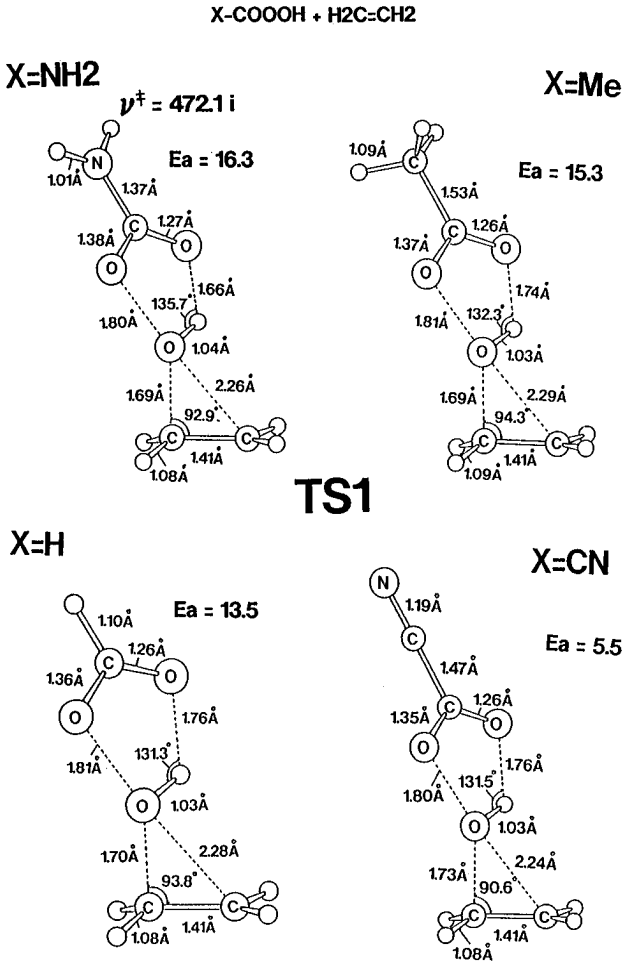

Figure 7. Effects of substituents attached to the peracid on transition-state geometries and MP4(SDTQ)/6-31G*//MP2/3-21G activation energies (in kcal/mol).

Figure 8 illustrates substituent effects of the olefins on TS1. As the substituent changes, X = NH_2 → Me → H → CN, E_a values increase significantly. Olefins work as electron donors as indicated by the Hammett $\rho = -1.3$ in Chart 1. The reaction between HCOOOH and

(13) There are no transition states between reactants and A and between C and products. Geometries of two intermediates A and C were obtained starting from those of the reactants and products, respectively, without any energy barriers.

(14) Free-energy changes ($\Delta G°$'s) of the following two equilibriia were evaluated by the use of thermochemical data in the Supporting Information.

$$\text{ethylene} + \text{performic acid} \overset{\Delta G°_1}{\rightleftharpoons} \text{the intermediate A}$$

$$\text{the intermediate C} \overset{\Delta G°_2}{\rightleftharpoons} \text{ethylene oxide} + \text{formic acid}$$

$\Delta G°_1 = +4.72$ kcal/mol and $\Delta G°_2 = -0.01$ kcal/mol were obtained under $T = 298$ K and $p = 1$ atm. The value of $\Delta G°_1$ indicates that the concentration of the intermediate A, [A], is quite small in the van't Hoff equation:

$$\Delta G° = -RT \ln K = -RT \ln[\text{A}]/([\text{ethylene}][\text{performic acid}])$$

That is, the inetermediate A is passed through rapidly and is not detectable. The almost zero value of $\Delta G°_2$ indicates that the concentration of the intermediate C is nearly equal to that of products under room temperature ($T = 298$ K). However, the step B → C is significantly exothermic,and the temperature is largely raised. Thus, the equilibrium is shifted to the product side, and the intermediate C is practically undetectable.

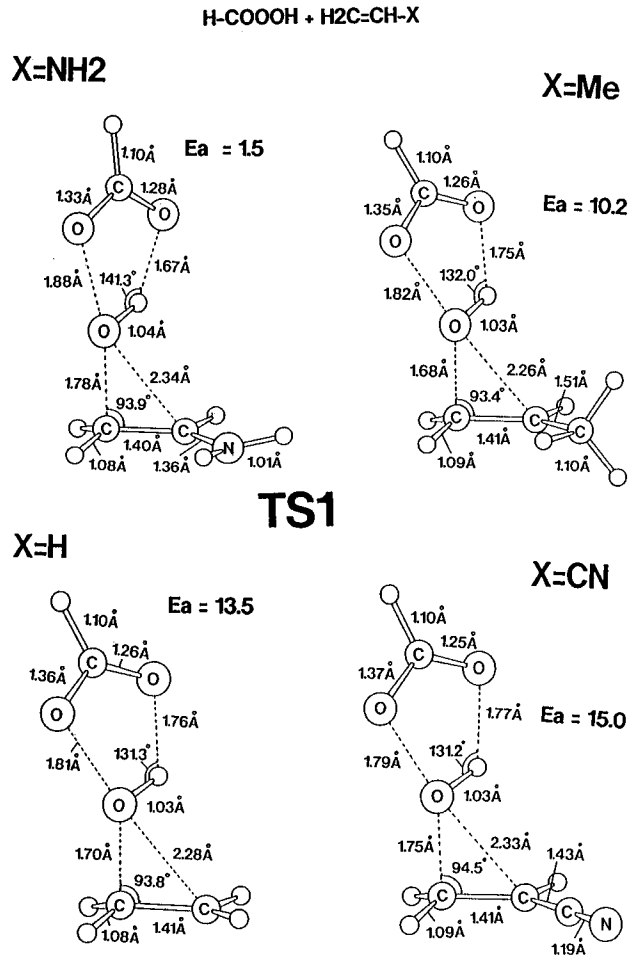

Figure 8. Effects of substituents attached to ethylene on transition-state geometries and MP4(SDTQ)/6-31G*//MP2/3-21G activation energies (in kcal/mol).

aminoethene (X = NH_2) is found to have a remarkably small activation energy, E_a = 1.5 kcal/mol. The propylene (X = Me) reaction has E_a = 10.2 kcal/mol, which is a typical energy for the peracid epoxidation of olefins.[15] Figure 8 also demonstrates that the TS1 geometry is insensitive to substituent changes.

IV. Concluding Remarks

This work dealing with the peracid epoxidation of olefins using *ab initio* calculations indicates the following:

(1) The first transition state (TS1) is formed in the rate-determinig step. Its geometry is surprisingly similar to that in Chart 1. The kinetic isotopic effect is well reproduced theoretically.

(2) The O−H bond of the peracid is retained in TS1.

(3) The retention gives rise to an unstable intermediate B.

(4) The intermediate is followed by the second transition state (TS2) for the proton transfer and the closure of the epoxide ring. TS2 has an extremely small activation energy.

(5) Substituent effects on activation energies of TS1 are quite large, reflecting the Hammett correlation. TS1 geometries are insensitive to substituents. The TS1 feature proposed in Chart 1 is valid regardless of substituents.

Acknowledgment. The authors thank the Information Processing Center of Nara University of Education for the allotment of the CPU time of the CONVEX C-220 computer and the Computer Center of Nara University for that of the CONVEX C-3420 computer.

Supporting Information Available: Z-matrices of the geometries of reactants, products, intermediates, and transition states, their vibrational frequencies, and thermochemical data (45 pages). This material is contained in libraries on microfiche, immediately follows this article in the microfilm version of the journal, and can be ordered from the ACS; see any current masthead page for ordering information.

JO941544K

(15) Hoveyda, A. H.; Evans, D. A.; Fu, G. C. *Chem. Rev.* **1993**, *93*, 1307.